

Wall shear stress in outflow tract premature ventricular contraction location assessed through 4D-flow MRI

Virgile Chevance ^{1,2}, Arshid Azarine ^{2†}, David A. Hamon ^{3,4†},
Tarvinder S. Dhanjal ⁵, Emmanuel Teiger ³, Jean-François Deux ^{1,6},
and Nicolas Lellouche ^{3*}

¹Radiology Department, Hopital Henri Mondor, APHP, Creteil, France; ²Radiology Department, Centre Chirurgical Marie Lannelongue, Groupe Hospitalier Paris Saint Joseph, Paris, France; ³Cardiology and Electrophysiology Unit, Hopital Henri Mondor, APHP, 51 Avenue du Marechal de Lattre de Tassigny, 94000 Creteil, France; ⁴University of Iowa Hospitals and Clinics (UIHC), Department of Cardiology, Carver College of Medicine, Iowa City, IA; ⁵Department of Cardiac Electrophysiology, University of Warwick, Gibbet Hill, Coventry, UK; and ⁶Radiology Department, University Hospitals of Geneva, Geneva, Switzerland

Received 30 November 2023; accepted after revision 22 January 2024; online publish-ahead-of-print 30 January 2024

Keywords

Cardiac imaging • 4D-flow MRI • Wall shear stress • Premature ventricular contraction • Right ventricular outflow tract

Premature ventricular contraction (PVC) is a frequent cardiac arrhythmia¹ and numerous electrophysiological causes have been proposed to explain PVC occurrence^{2,3}. However, the exact mechanistic origin of PVCs is unclear and the development of cardiac imaging particularly with cardiovascular magnetic resonance imaging (CMR)⁴ has shown that PVCs can be associated with underlying substrate abnormalities only diagnosed with CMR.

Chronically increased inhomogeneous wall shear stress (WSS) has been proposed as a possible factor implicated in right ventricular⁵ and left ventricular remodelling.⁶ This could potentially lead to PVCs by increasing fibrous content as has been shown in chronic dilated aortas with increased WSS.⁷

We conducted a prospective observational study with the aim of characterizing right ventricular outflow tract (RVOT) flow parameters, eccentricity and WSS with a 4D-flow MRI sequence. We correlated these markers with RVOT electrical amplitude abnormalities and PVC location, identified during 3D electroanatomical mapping ablation.

We included 10 patients who referred to our centre for RVOT PVC ablation. All underwent CMR before electroanatomical mapping. We also included a matched population (2:1) on age and sex of 20 patients who had previously undergone normal CMR with 4D-flow MRI from our database.

The study protocol was approved by a local ethics committee and the study was performed in accordance with the ethical principles stated in the Declaration of Helsinki. All subjects gave written informed consent to participate to our database.

Analysis of the CMR was performed on two dedicated softwares: CVi42 (Circle Cardiovascular Imaging; Calgary, Canada) and Arterys

(San Francisco, USA). The observers visually analysed in RVOT long-axis view and in 3D streamlines the laminarity of the flow (Y/N) using the method defined by Azarine *et al.*⁸ Flow eccentricity was assessed in the cross-sectional view of the RVOT based on whether flow was central (Y/N). Wall shear stress maps were centred on the subvalvular (pulmonary valve) region of the RVOT, in long-axis and in cross-sectional of the main AP axis view. The RVOT region was divided in six segments.

During the PVC ablation procedure, all patients underwent electroanatomic mapping using the CARTO 3 (Biosense-Webster) or Ensite Velocity (Abbott Laboratories) systems. Mapping was performed using either the Pentaray catheter (Biosense-Webster) or the HD grid catheter (Abbott Laboratories). RVOT also was divided in six anatomical segments. We measured before radiofrequency applications the mean ventricular electrogram (EGM) amplitude in sinus rhythm (SR) in each of these segments. Then, we retrospectively correlated the region of heterogeneity and PVC location with the lowest RVOT EGM amplitude to evaluate the local electrical remodelling.

The exact origin of PVC was defined as the site at which radiofrequency catheter ablation resulted in successful arrhythmia suppression.

The study population had a mean age of 54 years with 67% female patients. A minority had cardiovascular disease (20% had arterial hypertension and 30% a documented underlying cardiomyopathy). Premature ventricular contraction patients received beta-blockers in 50% of cases and Class IC antiarrhythmic drugs (flecainide) in 30% of cases.

Three patients had significant LV dilatation on CMR. Two patients had global LV systolic dysfunction and three patients had borderline

* Corresponding author. Tel: +33 1 49 81 43 50; fax: +33 1 49 81 28 83. E-mail address: nicolas.lellouche@aphp.fr

† These two authors contributed equally to the study.

© The Author(s) 2024. Published by Oxford University Press on behalf of the European Society of Cardiology.

This is an Open Access article distributed under the terms of the Creative Commons Attribution-NonCommercial License (<https://creativecommons.org/licenses/by-nc/4.0/>), which permits non-commercial re-use, distribution, and reproduction in any medium, provided the original work is properly cited. For commercial re-use, please contact journals.permissions@oup.com

Table 1 Comparison of PVC location on electrophysiological ablation mapping and area of highest WSS on 4D-flow MRI mapping in patients ($n = 10$)

Patients (n = 15)	PVC location on ablation map	Laminar flow (Y/N)	Vortex (Y/N)	Hyperpressure patch location on WSS maps	Lowest EGM amplitude RVOT segment (mean \pm SD in mV)	Colocalization WSS/PVC location (Y/N)	Colocalization WSS/lowest RVOT EGM (Y/N)
Patient 1	Anterior RVOT	Y	N	Postero-septal RVOT	Postero-septal (0.13 ± 0.06)	N	Y
Patient 2	Postero-septal RVOT	Y	N	Postero-septal RVOT	Postero-septal (0.6 ± 0.2)	Y	Y
Patient 3	Postero-septal RVOT	Y	N	Postero-septal RVOT	Antero-lateral (1.16 ± 0.87)	Y	N
Patient 4	Postero-septal RVOT	Y	N	Postero-septal RVOT	Posterior (0.25 ± 0.12)	Y	Y
Patient 5	Postero-septal RVOT	Y	N	Posterior RVOT	Posterior (0.6 ± 0.32)	Y	Y
Patient 6	Postero-septal RVOT	Y	N	Postero-septal RVOT	Postero-septal (1.05 ± 0.82)	Y	Y
Patient 7	Postero-septal RVOT	Y	N	Anterior RVOT	Anterior (0.04 ± 0.01)	N	Y
Patient 8	Postero-septal RVOT	Y	Y ^a	Antero-lateral RVOT	Antero-lateral (0.69 ± 0.34)	N	Y
Patient 9	Postero-septal RVOT	Y	N	Postero-septal RVOT	Postero-septal (0.33 ± 0.08)	Y	Y
Patient 10	Postero-septal RVOT	Y	N	Postero-septal RVOT	Postero-septal (0.37 ± 0.27)	Y	Y

EGM, electrogram; PVC, premature ventricular contraction; RVOT, right ventricle outflow tract; SD, standard deviation; WSS, wall shear stress.

^aDiastolic only.

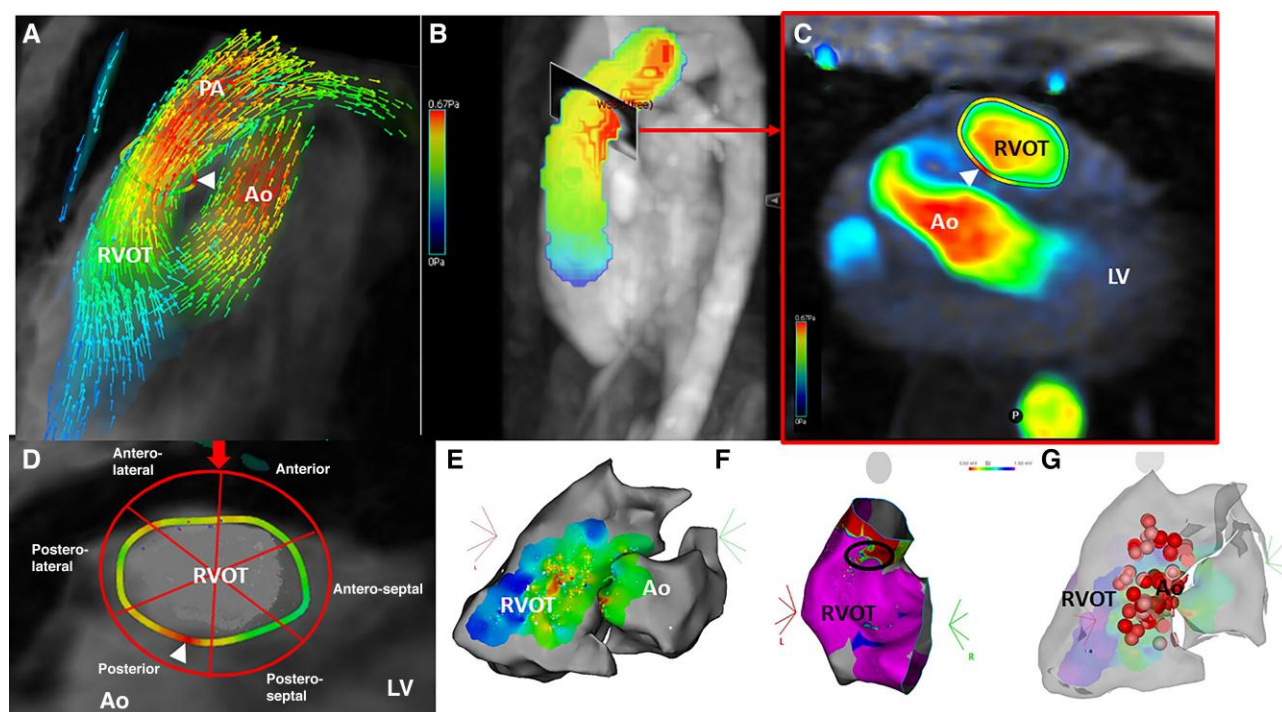


Figure 1 Illustration of the right ventricular ejection pathway segmentation method and correlation with electrophysiological findings. (A) Colorimetric streamline of the systolic flows in the aorta and the right ventricular ejection pathway. White arrowhead: position for the wall shear stress (WSS) analysis under the pulmonary annulus. (B) Colorimetric flow mapping in the RVOT and PA. Arrow: position for the analysis slice transverse to the main axis of the PA, under the pulmonary valve. (C) Transverse slice of the RVOT under the PA (position on B). Circumferential WSS analysis in colorimetric mapping. White arrowhead: area of relative heterogeneity of the WSS. (D) From the section obtained in C, red arrow, segmentation according to the six-segment method with the same angular arc of the subvalvular RVOT walls. Posterior adjacent to the aorta. Anterior proximal to the left internal mammary. Posterior and anterior septal on the LV side. Posterior and anterior lateral on the RV free wall side. White arrowhead: area of focal heterogeneity in WSS of the posterior-septal wall of the RVOT in this patient. (E and F) Colocalization on the same patient of the PVC focus on electrophysiological ablation maps with activation (E) and amplitude (F) map showing the common focus at the posterior-septal segment of the RVOT with the lowest EGM amplitude (black circle). (G) Final ablation map showing a colocalization with the WSS hyperpressure patch. Ao, aorta; LV, left ventricle; PA, pulmonary artery; RVOT, right ventricular outflow tract.

normal LVEF. One patient had RV dilatation, RV systolic dysfunction, and main pulmonary artery dilatation (34 mm diameter). All other patients ($n = 9$) had an RV of normal size and normal systolic function. Only one patient demonstrated myocardial necrosis evident as late gadolinium enhancement in four segments of the LV inferolateral and inferior median, lateral, and inferior apical.

In RVOT cross-sectional views, peak systolic blood flow was eccentric in all patients. Wall shear stress maps were heterogeneous, i.e. with focal areas of increased WSS, most often located in the postero-septal (7/10) and posterior (1/10) RVOT segments.

All controls had laminar RVOT flow with no vortex formation. In RVOT cross-sectional, peak systolic blood flow was eccentric in all but two controls. Those two controls had homogeneous WSS mapping in the perivalvular region of the RVOT. Remaining subjects exhibited areas of heterogeneity most often located on the posterior and postero-septal segments of the RVOT, similarly to PVC patients.

Premature ventricular contraction ablation catheter was successful in nine patients (90%). One procedure was considered as failure probably due to deep intramyocardial foci.

Colocalization analysis with the ablation regions demonstrated concordance with increased WSS zones in 7 of 10 patients (70%), in the posterior and postero-septal regions of the RVOT infundibulum (Table 1, Figure 1). As shown in the table, the region with the lowest EGM amplitude was perfectly concordant with the increased WSS zone in seven patients (70%), was the adjacent region to the increased WSS zone in two patients (20%), and was far from this zone in one patient (10%). These regions were concordant in 60% of cases with PVC location.

Idiopathic outflow tract PVC location is posterior and septal RVOT in ~80% of cases.⁹ It is still unclear why there is a predilection for PVC origin in these specific locations.

Flow eccentricity seemed to be the most likely explanation of WSS heterogeneity in our study.

Then, our results could suggest the development of a zone of frailty and subsequent arrhythmogenicity resulting from chronic relative hyperpressure at these foci. This relationship between hyperpressure, fibrosis, and vessel remodelling has already been shown in other studies: inhomogeneous WSS has been proposed as a possible factor implicated in right ventricular⁵ and left ventricular remodelling.⁶

This local remodelling could potentially lead to PVCs by increasing myocardial fibrosis content, as has been shown in chronic dilated aortas with increased WSS.⁷

RVOT PVC origin could be due to occult local remodelling that could be unmasked using advanced imaging technics and dense electrophysiological mapping. On the other hand, only 40% of our population developed PVCs on 'normal electrical tissue', representing what may be classified as the 'real' idiopathic PVC group.

Finally, as we found similar WSS results in patients and controls, other parameters should be of interest, like wall vessel rigidity, elastance modification, and/or systemic inflammation activation due to cardiovascular risk factors or local adipose tissue,¹⁰ generating local substrate remodelling to explain why chronic WSS would be responsible for local electrical remodelling or not.

Funding

No specific funding for this study.

Conflict of interest: none declared.

Data availability

All raw data included in this manuscript are available without limitations if necessary.

References

1. von Rotz M, Aeschbacher S, Bossard M, Schoen T, Blum S, Schneider S *et al*. Risk factors for premature ventricular contractions in young and healthy adults. *Heart* 2017;**103**: 702–7.
2. Gorennek B, Fisher JD, Kudaiberdieva G, Baranchuk A, Burri H, Campbell KB *et al*. Premature ventricular complexes: diagnostic and therapeutic considerations in clinical practice: a state-of-the-art review by the American College of Cardiology Electrophysiology Council. *J Interv Card Electrophysiol* 2020;**57**:5–26.
3. Natale A, Zeppenfeld K, Della Bella P, Kiu X, Sabbag A, Santangeli P *et al*. Twenty-five years of catheter ablation of ventricular tachycardia: a look back and a look forward. *Europace* 2023;**25**:eua225.
4. Berruezo A, Penela D, Jáuregui B, de Asmundis C, Peretto G, Marrouche N *et al*. Twenty-five years of research in cardiac imaging in electrophysiology procedures for atrial and ventricular arrhythmias. *Europace* 2023;**25**:eua2183.
5. Tsuchiya N, Nagao M, Shiina Y, Miyazaki S, Inai K, Murayama S *et al*. Circulation derived from 4D flow MRI correlates with right ventricular dysfunction in patients with tetralogy of Fallot. *Sci Rep* 2021;**11**:116–23.
6. von Knobelsdorff-Brenkenhoff F, Karunaharamoorthy A, Trauzeddel RF, Barker AJ, Blaszczyk E, Markl M *et al*. Evaluation of aortic blood flow and wall shear stress in aortic stenosis and its association with left ventricular remodeling. *Circ Cardiovasc Imaging* 2016;**9**:e004038.
7. Kiema M, Sarin JK, Kauhanen SP, Torniaainen J, Matikka H, Luoto ES *et al*. Wall shear stress predicts media degeneration and biomechanical changes in thoracic aorta. *Front Physiol* 2022;**13**:934–41.
8. Azarine A, Garçon P, Stansal A, Canepa N, Angelopoulos G, Silvera S *et al*. Four-dimensional flow MRI: principles and cardiovascular applications. *Radiographics* 2019;**39**:632–48.
9. Mont L, Seixas T, Brugada P, Brugada J, Simonis F, Rodriguez LM *et al*. Clinical and electrophysiologic characteristics of exercise-related idiopathic ventricular tachycardia. *Am J Cardiol* 1991;**68**:897–900.
10. Lu YY, Huang SY, Lin YK, Chen YC, Chen YA, Chen SA *et al*. Epicardial adipose tissue modulates arrhythmogenesis in right ventricle outflow tract cardiomyocytes. *Europace* 2021;**23**:970–7.